

CHAPTER (1)

INTRODUCTION

INTRODUCTION

1.1. Definition of corrosion

Corrosion [1] can be defined as the destruction of metals under the chemical or electrochemical action of the surrounding environment. All the corrosion reactions obey the thermodynamic laws. With the exception of noble metals like gold and platinum all other metals corrode and transform into substances similar to their mineral ores from which they are extracted. Corrosion can be simply defined as "the reverse process of extraction of metals".

1.2. Corrosion behavior of zinc in aqueous environment

1.2.1. What is zinc?

1.2.1.1. General properties [2]

Zinc has an atomic number of 30 and an atomic weight of 65.38. Its crystalline structure is hexagonal close-packed which determines physical and chemical properties. Zinc is an electro-positive element giving up two electrons for an oxidation state of +2. It is more reactive than brass, steel, nickel or copper but less so than aluminum or magnesium. The term reactive is relative and relates more to zinc's position on the electrochemical series at 0.76 volts to the standard hydrogen electrode.

In a normal atmosphere, zinc forms a basic zinc carbonate film that greatly retards its corrosion rate, which is similar to the aluminum oxide film that forms on aluminum which accounts for its low corrosion rate. Zinc when connected with metals below it in the electrochemical series will sacrificially protect that metal, which accounts for its wide usage in the galvanized steel industry.

1.2.1.2. Zinc protects steel in two ways

1. It is a barrier coating, and with its low corrosion rate offers extended life service.

2. It is sacrificial and protects the steel when exposed to the atmosphere. The sacrificial situation needs to be considered when coupling zinc to dissimilar metals.

Zinc is amphoteric and will form positive zinc ions in low pH solutions or negative zincate ions in high pH conditions and remain relatively insoluble in the neutral range. The lowest corrosion rates are encountered in the pH range of 6 to 10.5.

1.2.1.3. Zinc corrosion is controlled by four factors

1. Zinc has a high hydrogen overvoltage.
2. Zinc is attacked by acids at rates which decrease as pH increases.
3. Zinc is capable of forming insoluble basic salts when appropriate pH levels are reached (approximately 8).
4. Zinc is anodic to its metal impurities, to hydrogen and to most surface contaminants.

The mechanism for zinc corrosion is largely determined by the formation and stability of the basic carbonate film. Zinc reacts with oxygen to form zinc oxide (hydroxide) with subsequent reaction with carbon dioxide and water to form the basic carbonate ($\text{ZnO}/\text{CO}_3 \text{ Zn (OH)}_2$). Once this film is formed, the surface becomes passivated to further attack.

The atmosphere and location in which the material is used as well as weathering, rates of oxygen diffusion, wet/dry conditions, etc. will all have a bearing on corrosion rate. The composition of zinc seldom has a significant

effect on its rate of corrosion in atmospheric exposure. It is probable that all commercial forms of zinc have within plus or minus 10% of the same corrosion rate in any given outdoor environment.

1.3. Classification of corrosion

All metal consist of atoms having valency electrons which can be donated or shared. In a corrosive environment the components of the alloy get ionized and the movement of the electrons sets up a galvanic or electrochemical cell which causes oxidation, reduction, dissolution or simple diffusion of the elements.

The metallurgical approach of corrosion of metals is in terms of the nature of the alloying characteristics, the phases existing and their inter-diffusion under different environmental conditions. In fact, the process of corrosion is a complex phenomenon and it is difficult to predict the exclusive effect or the individual role involved by any one of the above mentioned processes.

Based on the above processes, corrosion can be classified in many ways as low temperature and high temperature corrosion, direct oxidation and electrochemical corrosion, etc. The preferred classification is:

- (i) Dry or chemical corrosion, and.
- (ii) Wet or electrochemical corrosion.

Dry corrosion occurs in the absence of a liquid phase or above the dew point of the environment. Vapors and gases are usually coordinates; it is often associated with high temperature. An example is the attack of steel by furnace gases .Wet corrosion occurs when a liquid is present in contact with the metal. This occurs in aqueous solutions or electrolytes. A common example is corrosion of steel by water.

The nature and extent of corrosion depend on the metal and the environment. The important factors which may influence the corrosion process are:

- (i) Nature of the metal, (ii) nature of the environment,
- (iii) Electrode potential, (iv) temperature,
- (v) solution concentration, (vi) aeration,
- (vii) agitation, (viii) pH of the solution and
- (ix) nature of the corrosion products.

1.3.1. Various forms of corrosion [3]

Corrosion can manifest itself in the following main forms:

1.3.1.1. General corrosion or Uniform attack

This is the most common type in which the corrosion is uniform over the entire exposed surface. an example of this is water tank exposed to the atmosphere.

1.3.1.2. Pitting or Localized attack

It is one of the most destructive and insidious forms of corrosion. It is a highly localized corrosion; the attack is being limited to extremely small areas. An example is the corrosion of stainless steels in chloride solutions.

1.3.1.3. Galvanic corrosion

It is an accelerated electrochemical action due to two different metals being in electrical contact and exposed to an electrolyte. Heat exchanger failure in which aluminum tubes are supported by a perforated steel sheet is an example of this type of corrosion.

1.3.1.4. Crevice corrosion

This type of corrosion takes place when only one metal is in contact with different concentrations of the environment. Rectangular metal containers and reverted lap joints offer the possibility for this type of corrosion.

1.3.1.5. Stress corrosion

It is the spontaneous cracking resulting from the combined effect of prolonged stress and corrosive attack. Caustic embrittlement of boilers provides an example for this type of corrosion.

1.3.1.6. Erosion – corrosion

It is the acceleration in the rate of attack of a metal because of the relative movement between a corrosive fluid and the metal surface. Heat exchanger tubes with water movement undergo this type of corrosion.

1.3.1.7. Fretting corrosion

It is a case of deterioration resulting from repetitive rumbling at the interface between two surfaces in a corrosive environment. It is found in aircraft engine parts.

1.3.1.8. Filiform corrosion

It is a special type of rusting which occurs on certain metals under protective films like paints and is characterized by a thread like growth. Filiform corrosion may be found on tools coated with oil films, refrigerator doors etc.

1.4. Corrosion inhibitors

1.4.1. Definition

An inhibitor is "A substance which retards corrosion when added to an environment in small concentrations"[4]. Inhibitor may also be defined on an electrochemical basis as substances that reduce the rates of either or both of partial anodic oxidation/ or cathodic reduction reaction. Also corrosion inhibitors are chemical substances which added in small amounts to the environment will reduce the corrosion rate of the metals and their alloys [5-7].

1.4.2. Classification of corrosion inhibitors

The corrosion inhibitors are classified according to the environment, mode of action and composition of the inhibitors. The inhibitors are classified as acidic inhibitors, neutral inhibitors, alkaline inhibitors, and vapor phase inhibitors according to the environments in which they find applications

Inhibitors can also be classified as anodic [8, 9], cathodic [10], and mixed-type [11] inhibitors depending on the mechanism of their inhibiting action on the electrochemical corrosion. Other classifications like passivators, precipitate inhibitors and adsorbents are also in use. Depending on the nature of the inhibitors they can also be classified as organic or inorganic inhibitors [12-14]. The different modes of inhibiting electrode reactions have been analyzed by Fischer [15] and distinguished among various mechanisms of action such as (i) interface inhibition, (ii) electrolyte layer inhibition, (iii) membrane inhibition, and (iv) passivation. Subsequently, Lorenz and Mansfield proposed a clear distinction between interface and interphase inhibition. They proposed two different types of retardation mechanisms of electrode depending on types of reaction including corrosion. Interface inhibition presumes a strong interaction between the inhibitors and the surface of the metal. In this case the inhibitor adsorbs as a potential dependent two-dimensional layer. Interphase inhibition

presumes a three dimensional layer between the corroding substrate and the electrolyte [16-20]. Such 3-dimensional layer generally consists of weakly soluble compounds such as oxidized corrosion products or inhibitor forming porous layers. The inhibition efficiency depends strongly on the three dimensional layers especially its porosity and solubility.

1.4.3. Corrosion rate measurements

Recently the measurement of corrosion rates in the presence of corrosion inhibitors by weight-loss and electrochemical methods have been reviewed by Mercer [21].

1.4.3.1. Chemical method

i) Weight-loss measurements

The efficiency of inhibition was calculated from the weight loss values using the following equation:

$$\% \text{ IE} = \frac{W_{\text{free}} - W_{\text{add}}}{W_{\text{free}}} \times 100 \quad (1.1)$$

where, W_{free} = weight loss in the corrosive medium in mg cm^{-2} .

W_{add} = weight loss in the inhibited solutions in mg cm^{-2} .

ii) Hydrogen evolution method

The efficiency of a given inhibitor can be evaluated as the percentage reduction in reaction rate (K), so the percentage inhibition efficiency (% IE) can be calculated, as follows:

$$\% \text{ IE} = \frac{K_{\text{free}} - K_{\text{add}}}{K_{\text{free}}} \times 100 \quad (1.2)$$

where, K_{free} = specific reaction rate in the corrosive medium.

K_{add} = specific reaction rate in the inhibited solutions.

Specific reaction rate constants are calculated from the relation:

$$V = Kt \quad (1.3)$$

where, V = volume of hydrogen evolved in cm^3 .

t = time in min.

iii) Thermometric method

A simple rapid and limited method for comparing the inhibition efficiency of different additional agents [22]. A reaction number, R.N., is defined by Mylius **as**:

$$\text{R.N.} = \frac{T_m - T_i}{t} \text{ } ^\circ\text{C} / \text{min} \quad (1.4)$$

where, T_m = maximum temperature in K.,

T_i = initial temperature in K.

t = time in min. from the start of the experiment to attained T_m .

The reaction number is proportional to the rate of the corrosion of the metal. The extent of corrosion inhibition by a certain concentration of a particular additive is evaluated from the percentage reduction in the reaction number

$$\% \text{ Reduction in R.N.} = \frac{(\text{R.N.})_{\text{free}} - (\text{R.N.})_{\text{add.}}}{(\text{R.N.})_{\text{free}}} \times 100 \quad (1.5)$$

where, $(\text{R.N.})_{\text{free}}$ = reduction in R.N. in the corrosive medium.

$(\text{R.N.})_{\text{add.}}$ = reduction in R.N. in presence of additive.

1.4.3.2. Electrochemical methods

i) Open-circuit potential method

This method is used to measure the steady state potential, (E_{OCP}), of the metal or alloy in the absence and presence of additives [23]. In this method, the potential of the corroding material is measured against reference electrode at different time intervals until a steady state is reached.

ii) Potentiodynamic polarization method

a) Tafel plots

In this method corrosion current can be determined from polarization curves by intercept method based on anodic and/or cathodic Tafel curves.

The intercept method [24, 25] used in the present work for the determination of corrosion current is performed by extrapolating the Tafel lines to the experimentally was measured free corrosion potential. The corresponding $\log i_{\text{corr}}$ value was obtained by interception and i_{corr} then evaluated.

b) Linear polarization method

This technique is an accepted method of monitoring corrosion rates [26-29]. For a corroding electrode, the polarization resistance R_p , at small applied range of potential or current, is related to the corrosion current density, and i_{corr} , calculated by the following equation

$$i_{\text{corr}} = \frac{b_a b_c}{2.3(b_a + b_c)} \cdot \frac{1}{R_p} = \frac{B}{R_p} \quad (1.6)$$

where, b_a = anodic Tafel slope.

b_c = cathodic Tafel slope.

R_p = is the polarization resistance.

A controlled potential scan is applied over a small range, typically ± 25 mV with respect to E_{corr} , at a scan rate of 0.1 mV/sec. The resulting current is plotted against the potential. The slope of this linear potential – current plot at E_{corr} , is identical with the polarization resistance which used together with the measured Tafel constants to determine the corrosion rate.

The percentage inhibition efficiency (%IE) can expressed as:

$$\% \text{ IE} = \frac{i_{\text{free}} - i_{\text{add}}}{i_{\text{free}}} \times 100 \quad (1.7)$$

where, i_{free} = corrosion current in the corrosive medium.

$i_{\text{add.}}$ = corrosion current in presence of additive.

iii) Impedance method

In recent years, the impedance technique has been widely used for measuring the corrosion rates of metals. The main advantage of this method is the complete elimination of the solution resistance. The equivalent circuit of a corroding metal which has both anodic and cathodic reactions under activation control may be represented as a parallel combination of charge transfer resistance (R_t) and double layer capacitance (C_{dl}) and the solution resistance (R_s) is in series.

From the R_t value, the i_{corr} is obtained from the relationship:

$$i_{\text{corr.}} = \frac{b_a \times b_c}{2.303(b_a + b_c) \times R_t} \quad (1.8)$$

The impedance of the above circuit for the given ω ($\omega = 2\pi f$) is:

$$Z = R_s + \frac{1}{j\omega C_{dl} + \frac{1}{R_t}} \quad (1.9)$$

$$Z = \frac{R_t}{1 + \omega^2 C_{dl}^2 R_t^2} - \frac{j\omega C_{dl} R_t^2}{1 + \omega^2 C_{dl}^2 R_t^2} \quad (1.10)$$

$$Z = Z' - jz'' \quad (1.11)$$

This method gives the instantaneous corrosion rate. This technique can be used in low and high resistive media.

Two main plots formats are frequently used in impedance due to presentation, the Nequist and Bode plots. There are also some other plots which enable interpretation of diffusion phenomena or specific electrochemical process [30].

a) The Nyquist plot

In this plot the imaginary component, Z'' is plotted against the real component, Z' at each excitation frequency. But the frequency is not presented on the plot. In the ideal case the plot is in the form of semicircle as shown in Fig. (1.1), from this figure, at high frequencies, the impedance of the Randles cell was almost entirely created by the ohmic resistance R_s or R_Ω , the frequency reaches its high limit at the left most of the semicircle, where the semicircle touches the x axis (real component). At the low frequency limit, the Randles cell also approximates a pure resistance, but the value is $(R_s + R_p)$. The frequency reaches its low limit at the right most end of the semicircle. R_s can be determined from the frequency independent limit of $|Z|$ at high frequencies and $(R_s + R_p)$ from the corresponding limit at low frequencies.

The double layer capacitance, C_{dl} can be determined from the value of the angular frequency at maximum Z'' (ω_{max}) and the polarization resistance according to:

$$C_{dl} = \frac{1}{\omega_{max} R_p} = \frac{1}{2\pi f_{max} R_p} \quad (1.12)$$

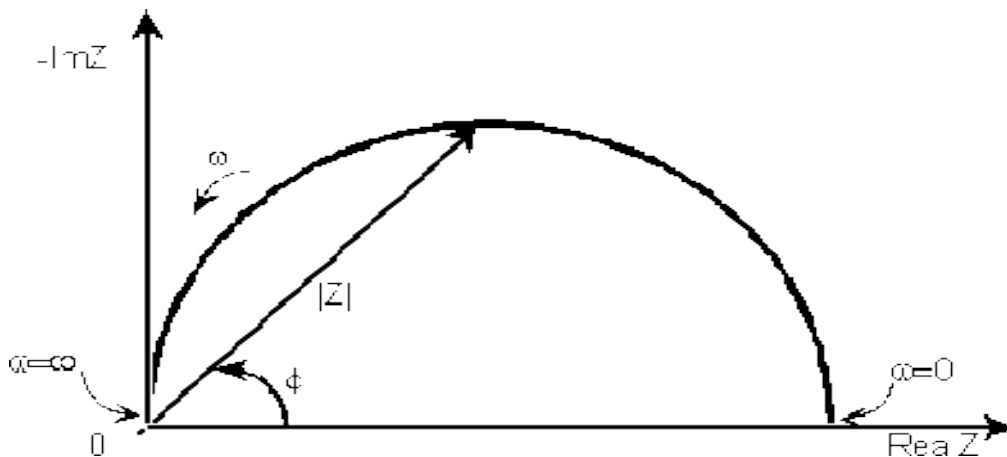


Fig. (1.1): Nyquist plot with impedance vector.

The figure shows that low frequency data are on the right side of the plot and higher frequencies are on the left. This is true for EIS data where impedance usually falls as frequency rises (this is not true of all circuits).

b) Bode plot

The impedance is plotted with log frequency on the x-axis and both the absolute value of the impedance ($|Z| = Z_0$) and phase-shift on the y-axis. Unlike the Nyquist plot, the Bode plot explicitly shows frequency information as shown in Fig.(1.2).

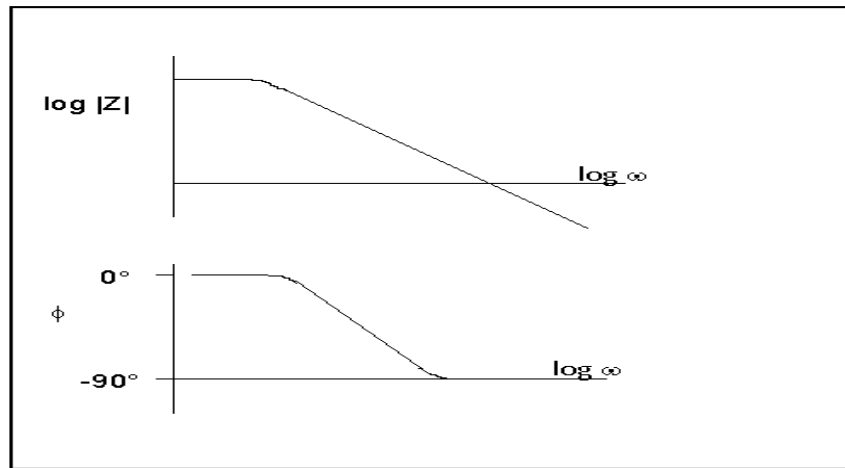


Fig.(1.2): Bode Plot with One Time Constant

In this plot, the absolute impedance $|Z|$, as calculated by the equation:

$$|Z| = [(Z')^2 + (Z'')^2]^{0.5} \quad (1.13)$$

And the phase shift, θ° , are plotted as a function of the frequency, f . the $\log |Z|$ vs. $\log f$ presentation had some distinct advantage over the Nyquist plot. It enables a wide range of measurements over orders of frequency magnitude (from 10^{-2} to 10^5 Hz) and shows the dependence of the electrode impedance on the frequency on a direct look. The $\log |Z|$ vs. $\log f$ curve can yield values of R_p and R_s . At the highest frequencies shown in Fig.(1.2) the ohmic resistance

dominates the impedance and $\log R_s$ can be read from the higher frequency horizontal plateau at the lowest frequencies, polarization resistance also contributes and $\log (R_p + R_s)$ can be read at the low frequency horizontal plateau. At intermediate frequencies, this curve is a straight line with a slope of (-1). Extrapolating this line to $\log |Z|$ axis at $\omega = 1$ ($\log \omega = 0$ at $f = 0.16$ Hz) yields the value of C_{dl} from the equation:

$$|Z|_{0.16\text{Hz}} = \frac{1}{C_{dl}} \quad (1.14)$$

The Bode plot also shows the phase angle, θ . At the high and low frequency limits, where the behavior of Randles cell is resistor-like, the phase angle is nearly zero. At intermediate frequencies, θ , increases as the imaginary component of the impedance increase. The θ vs. $\log f$ plot yields a peak at which the phase shift of the response is maximum.

To calculate the corrosion rate, one must determine the corrosion current (i_{corr}), and to determine i_{corr} . From polarization resistance, the Tafel constants are needed. Equation (1.8) shows the relationship between the R_t value, the Tafel constants and the corrosion current.

vi) Electrochemical frequency modulation method

Electrochemical frequency modulation (EFM) is a new technique provides a new tool for electrochemical corrosion monitoring. In this technique, a potential perturbation by two sine waves of different frequencies is applied to a corroding system. As corrosion process is non- linear in nature, responses are generated at more frequencies than the frequencies of the applied signal. The current responses can be measured at zero, harmonic, and inter modulation frequencies.

Analysis of these current responses can result in the corrosion current density and Tafel parameters. Electrochemical frequency modulation is nondestructive technique as electrochemical impedance (EIS) that can directly and rapidly give values of the corrosion current without a prior knowledge of Tafel constants. The great strength of the EFM is the causality factor, which serves as an internal check on the validity of the EFM measurement. With the causality factors the experimental EFM data can be verified [31,32]. Identical cell assembly as used in both polarization and impedance studies was used for Electrochemical frequency modulation (EFM) measurement. Experiments were carried out using potential amplitude 10mV for both frequencies 2 and 5 Hz. All electrochemical experiments were carried out using Gamry PCI300/4 Potentiostat / Galvanostat / Zra analyzer, DC105 Corrosion software, EIS300 Electrochemical impedance spectroscopy software, EFM140 electro chemical frequency modulation software and echem analyst 5.21 for results plotting, graphing, data fitting & calculating.

1.5. Literature Survey on Corrosion Inhibition of Zinc in Aqueous Solutions

The inhibiting action of 2-mercaptobenzimidazole on the corrosion of zinc in phosphoric acid (H_3PO_4) solution was investigated by weight loss and polarization [33]. The result reveals that the inhibitor is effective for the inhibition of zinc in H_3PO_4 solution and retards the anodic and cathodic corrosion reactions with emphasis on the former (mixed inhibitors).

Ethoxylated fatty alcohols with different numbers of ethylene oxide units were tested as corrosion inhibitors for dissolution of zinc in hydrochloric acid using weight loss and galvanostatic polarization measurements [34] .The inhibition efficiency was found to increase with increasing concentration,

number of ethylene oxide units per molecule and with decreasing temperature. Inhibition was explained on the basis of adsorption of ethoxylated fatty alcohols molecules on the metal surface through their ethoxy group. The degree of surface coverage varied linearly with logarithm of inhibitor concentration Fitting Temkin isotherm.

The action of some organic compounds from the group of surfactants and polyethylene glycols (PEGs) on the corrosion of zinc in alkaline media was studied [35]. The investigations were carried out by use of electrochemical and nonelectrochemical methods. The effectiveness of the inhibitors was compared and it was found that the PEG of average molecular weight 400 (PEG400) was especially effective. The assumption has been advanced that zinc corrodes electrochemically in the first stage of exposition, but the chemical corrosion prevails after a longer time.

The inhibition of zinc corrosion in an aerated 0.5 M NaCl solution by environmentally acceptable cation inhibitors, Al^3 , La^3 , Ce^{3+} and Ce^{4+} was studied [36]. The inhibition efficiencies of these cations were determined by polarization measurements of a zinc electrode in the solution. The efficiencies of Ce^{3+} and La^{3+} were high, more than 90% but those of other cations were negative, indicating stimulation of zinc corrosion. X-ray photoelectron spectra for the zinc surface treated in the solution containing Ce^{3+} revealed that a thick protective layer composed of $\text{Ce}(\text{OH})_3$, Ce_2O_3 and small amounts of $\text{Zn}(\text{OH})_2$ and ZnO formed on the surface and there was no chloride ion within the layer. Processes of the layer formation on the surface were discussed based on these results.

Cerium(III) chloride (CeCl_3) is an effective inhibitor for corrosion of zinc in an aerated 0.5 M NaCl solution by the formation of a thick film composed of cerium-rich oxide and hydroxide [37]. In this study, a protective

film was prepared by treatment of a zinc electrode in an aqueous solution of 1×10^{-3} M Ce (NO₃)₃ at 30 °C for 30 min and examined in an aerated 0.5 M NaCl solution at 30°C by polarization measurements after immersion of the electrode in the NaCl solution for 4–240 h. The film comprised oxides and hydroxides of Ce (III) and Ce (IV) ions mostly. The protective efficiency of the film against zinc corrosion was maintained remarkably high, more than 91% during immersion in 0.5 M NaCl for 240 h. Little pitting corrosion was observed on the electrode surface. However, this film could not heal the scratched surface of zinc electrode in the NaCl solution.

Effects of some organic inhibitors e.g. [sodium benzoate (NaBz), sodium N-dodecanoylsarcosinate (NaDS), sodium S-octyl-3-thiopropionate (NaOTP), 8-quinolinol (8-QOH) and 1,2,3-benzotriazole (BTAH)] on corrosion of zinc in an aerated 0.5 M NaCl solution were investigated by polarization measurements [38]. The inhibition was explained in terms of formation of precipitate films of Zn(II) salts or complexes on the zinc surface together with zinc hydroxide and oxide to prevent corrosion in the solution. High inhibition efficiencies of NaOTP were acquired at concentrations $C = 1 \times 10^{-6} - 3 \times 10^{-5}$ M, BTAH at $C = 1 \times 10^{-4} - 1 \times 10^{-3}$ M, 8-QOH at $C = 1 \times 10^{-3} - 3 \times 10^{-3}$ M and NaBz at $C = 3 \times 10^{-3} - 1 \times 10^{-2}$ M. The film formed on the zinc surface was analyzed by X-ray photoelectron and Fourier transforms infrared reflection spectroscopies.

New surface treatment of zinc, called "carboxylting", which could be an environmentally friendly alternative to the usual conversion treatments [39]. Carboxyl ting requires use of both n-alkyl carboxylic acid and peroxoborate as oxidizing agent, in a water–ethanol mixture. As in the phosphating process, the carboxylating one is carried out in four steps: the activation step, oxidation of the zinc substrate at an acidic pH, germination and growth of zinc carboxylate crystals. Influence of the activator content, treatment time, oxidizing agent

concentration, and chain length of the carboxylic acid was successively examined. Carboxylates covered zinc samples were tested in corrosion conditions. The longer the carbon chain length, the more corrosion resistant the coating; its layered structure easily allows exchanging anions and a hydroxocarboxylate of zinc is stabilized during the corrosion test then delays the white rust formation.

The synergistic inhibition effects of cerium(III) chloride, CeCl_3 and sodium silicate, $\text{Na}_2\text{Si}_2\text{O}_5$ (water glass) on corrosion of zinc in an aerated 0.5M NaCl solution at 30°C were examined by polarization measurements [40]. Equimolar mixtures of these inhibitors were markedly effective, indicating that the inhibition efficiencies of the mixture at 1×10^{-4} of each inhibitor were 95.9 % and 93.6 % after immersion of a zinc electrode in the solution for 3 and 120h., respectively. X-ray photoelectron spectra revealed that a protective layer composed of hydroxylated or hydrated cerium-rich oxide and small amounts of zinc hydroxide and silicate formed on the zinc surface. A high inhibition efficiency of 1×10^{-3} M $\text{Na}_2\text{Si}_2\text{O}_5$, 97.7 % was obtained for corrosion of a zinc electrode which was previously treated in the NaCl solution of 1×10^{-3} M CeCl_3 at 30°C for 30 min.

Cerium(III) chloride, CeCl_3 and sodium octyothiopropionate $\text{C}_8\text{H}_{17}\text{S}(\text{CH}_2)_2\text{COONa}$ (NaOTP) are effective inhibitors for zinc corrosion in 0.5M NaCl. Synergistic inhibition of zinc corrosion in an aerated 0.5M NaCl solution by a mixture of these inhibitors was investigated by polarization measurements after immersion of a zinc electrode in the solution for many hours [41]. The inhibition efficiency of 1×10^{-4} M CeCl_3 plus 1×10^{-5} M NaOTP mixture was high, 95.1% after both 3h. and 120 h. X-ray photoelectron spectroscopy and electron –probe microanalysis for the inhibited electrode revealed that the zinc surface was covered with a protective film composed of a hydrated or

hydroxylated Ce-rich oxide, a small amount of $\text{Zn}(\text{OH})_2$ and a trace of $\text{Zn}(\text{OTP})_2$ chelate. The inhibition effect of $1 \times 10^{-5} \text{ M}$ NaOTP in the NaCl solution for the zinc electrode previously treated in $1 \times 10^{-3} \text{ M}$ CeCl_3 for 30 min was also examined, indicating higher inhibition efficiency, 96.3% after immersion of the electrode in the solution for 120h.

A self-assembled monolayer (SAM) of hexadecanoate ion $\text{C}_{15}\text{H}_{31}\text{CO}_2^-$ (C_{16}A^-) was prepared on a zinc electrode covered with a layer of hydrated cerium(III) oxide Ce_2O_3 . The protection of zinc against corrosion was examined for the electrode coated with the Ce_2O_3 layer and the C_{16}A^- SAM in an oxygenated 0.5M NaCl solution [42]. A more positive open-circuit potential of the coated electrode was maintained during immersion in the solution for 4h. than that of the uncoated one and polarization curves showed marked suppression of the anodic process, implying that the layer was extremely high, more than 99%. The zinc surface coated with the Ce_2O_3 layer and the C_{16}A^- SAM was characterized by X-ray photoelectron and FTIR reflection spectroscopies and contact angle measurement with a drop of water.

The influence of oxide surface charge on the corrosion performance of zinc metals was investigated [43]. Oxidized zinc species (zinc oxide, zinc hydroxyl chloride, zinc hydroxyl sulfate and zinc hydroxyl carbonate) with chemical compositions similar to those produced on zinc during atmospheric corrosion are formed as particles from aqueous solution, and as passive films deposited onto zinc powder, and rolled zinc surfaces. Synthesized oxides are characterized by X-ray diffraction, Fourier transform infrared spectroscopy, scanning electron microscopy and electron probe X-ray micro analysis. The zeta potentials of various oxide particles, are determined by micro electrophoresis, are reported as a function of pH. Particulates containing a majority of zinc hydroxyl carbonate and zinc hydroxyl sulfate crystallites are found to possess a

Introduction

negative surface charge below pH 6, whilst zinc oxide- hydroxide and zinc hydroxyl chloride crystallites possess isoelectric points (IEP's) higher than pH 8. The ability of chloride species to pass through a bed of 3 ml diameter zinc powder is found to increase for surface possessing carboxyl and sulfate surface species, suggesting that negatively charged surface can aid in the repulsion of chloride ions. Electrochemical analysis of the open-circuit potential as a function of time at a fixed pH 6.5 showed that the chemical composition of passive films on zinc plates influences the ability of chloride ions to access anodic sites for periods of approximately 1h.

The influence of alloying elements on the corrosion behavior of rolled zinc sheet in aqueous media has been investigated by means of electrochemical techniques [44]. All the change in corrosion behavior seen in this study could be attributed to modification of the formation or stability of the passivating oxide film on the zinc surface. A low concentration of copper (0.6wt.%) inhibits the formation of the passivating film and reduces the stability of the film. Conversely, a low concentration of chromium (0.5wt.%) accelerates the passivation process and raises the stability of the film. The passivation and corrosion behavior shown by a commercially produced ternary alloy containing copper and titanium additions is almost the same as the behavior shown by model binary alloy containing only copper. The results obtained in this study are consistent with the hypothesis that alloying elements alter the electron-conducting and /or ion –conducting properties of the passivating oxide film.

The corrosion rate of zinc metal in aqueous solutions of potassium hydroxide was followed in time by measuring the amount of evolved hydrogen [45]. The zinc samples were pretreated with either mono benzyl amine, dibenzyl amine, tri benzyl amine or sulphonated benzyl amine. The hydroxide concentration was varied from 1 to 10 N. It was shown that the amines act either

as corrosion inhibitors or activators, depending on the KOH concentration and the duration of exposure which lasted up to 150 hrs.

Effects of NaCl and NH_4Cl on the initial atmospheric corrosion of zinc are investigated via quartz crystal microbalance (QCM) in laboratory at 80% RH { Relative Humidity} and 25°C [46]. The results showed that both NaCl and NH_4Cl can accelerate the initial atmospheric corrosion of zinc. The combined effect NaCl and NH_4Cl on the corrosion of zinc is greater than that caused by NH_4Cl and less than that caused by NaCl. Fourier transform infrared spectroscopy (FTIR), X-ray diffraction(XRD), Scanning electron microscopy (SEM) and Electron dispersion X-ray analysis (EDAX) are used to characterize the corrosion products of zinc. $(\text{NH}_4)_2\text{ZnCl}_4$, $\text{Zn}_5(\text{OH})_8\text{Cl}_2 \cdot \text{H}_2\text{O}$ and ZnO present on zinc surface in the presence of NH_4Cl while $\text{Zn}_5(\text{OH})_8\text{Cl}_2 \cdot \text{H}_2\text{O}$ and ZnO are the dominant corrosion products on NaCl treated zinc surface.

A comparison between the potentiodynamic behavior of the stationary and the rotating Zn disc electrodes in naturally aerated and de-aerated 0.1 M KClO_4 solution is performed [47]. The voltammograms of the stationary electrode in both solutions exhibited one anodic peak and two cathodic peaks. The anodic peak is replaced by two mass transport controlled O_2 reduction cathodic current plateaus in the forward scan by rotating the electrode in naturally aerated solutions. However, the reverse scan is characterized by only one cathodic peak observed at a potential depends on the experimental conditions. The more cathodic reduction peak referred to the reduction of the passive layer and split into two peaks at low scan rates. Interpretation of these data is made adopting a multi-path mechanism and a two layer passive film model. A correlation between the ClO_4^- and dissolved O_2 reduction and the thickness of the two passive layers is performed. The protective nature of the passive layers forms in different experimental conditions

is found to decrease with rotating the electrode and de-aerating the solution. Chronopotentiometry and electrochemical impedance measurements are also used in this study. Impedance technique shows a change in the ZnO thickness with the experimental conditions as a result of changing the reactions occurring in the electrode vicinity.

The influence of some hydrazide derivatives as corrosion inhibitors for zinc in 2M sodium hydroxide solution has been studied using weight loss and galvanostatic polarization technique [48]. In general, at constant acid concentration, the inhibitor efficiency increases with increase of concentration of inhibitor and decrease with rise in temperature. Polarization studied reveals that these compounds behave as mixed inhibitors. The effect of temperature was studied and activation energies were calculated and some thermodynamic activation parameters are calculated and discussed. The inhibition process can be explained in view of adsorption on the zinc surface. The adsorption of the inhibitors on zinc surface is found to obey Temkin adsorption isotherm. Addition of Ca^{2+} , Sr^{2+} , Ba^{2+} and Mg^{2+} ions to the alkaline medium containing the hydrazide derivatives increases the inhibition efficiency of the system.

The corrosion inhibition of zinc in hydrochloric acid by extract of *Nypa Fruticans Wurmb* was studied using weight loss techniques [49]. Maximum inhibition efficiency (and surface coverage) is obtained at an optimum concentration. However increase in temperature decreases the inhibition efficiency. The inhibition action of *Nypa Fruticans Wurmb* extract compared closely to that of 1,5-Diphenyl Carbazone (DPC). Optimum inhibition efficiency for zinc in the presence of *Nypa Fruticans Wurmb* extract is 36.43% and 40.70% with DPC. The phenomenon of physical adsorption has been proposed from the activation energy values ($19.33 \text{ kJ.mol}^{-1}$ and $21.11 \text{ kJ.mol}^{-1}$)

with *Nypa Fruticans* Wurmb extract and DPC respectively. A first order kinetics has been deduced from the kinetic treatment of the results.

The zinc metal surface is chemically modified by newly synthesized Schiff's bases and its corrosion protection was investigated [50]. The influence of increasing concentration of Schiff's bases on modification of zinc surface and immersion time in treatment bath are investigated and optimized for maximum corrosion protection efficiency. The electrochemical studies of treated zinc specimens are performed in aqueous acid solution using galvanostatic polarization technique. The treated zinc samples show good corrosion resistance. The recorded electrochemical data of chemically treated samples indicate a basic modification of the zinc surface. The protection efficiency of organic layer formed on zinc surface is tested by varying the acid concentration and temperature of the corrosive medium. The corrosion protection efficiency increases with the concentration of Schiff's bases and immersion time. This is due to a strong interaction between zinc and the organic molecules, which results in the formation of a protective layer. This layer prevents the contact of aggressive medium with the zinc surface. The surface modification is confirmed by the scanning electron microscopy images. The interaction between metal atoms and Schiff's bases is also established by IR studies.

The surface treatment of zinc and its corrosion inhibition was studied [51] using a product formed in the reaction between benzaldehyde and thiosemicarbozide (BTSC). The corrosion behavior of chemically treated zinc surface was investigated in aqueous chloride-sulphate medium using galvanostatic polarization technique. Zinc samples treated in BTSC solution exhibited good corrosion resistance. The measured electrochemical data indicated a basic modification of the cathode reaction during corrosion of treated zinc. The corrosion protection may be explained on the basis of adsorption and formation

of BTSC film on zinc surface. The film was binding strongly to the metal surface through nitrogen and sulphur atoms of the product. The formation of film on the zinc surface was established by surface analysis techniques such as scanning electron microscopy (SEM-EDS) and Fourier transform infrared spectroscopy (FTIR).

The electrochemical behavior of pure Zn and galvanized steel in solutions simulating the pore solution of carbonated concrete was studied by means of potentiodynamic polarization tests and polarization resistance measurements [52]. Pure Zn was chosen because it simulates well the behavior of galvanized steel, yielding more reproducible results. The effect of different degrees of carbonation and the presence of different chloride contents in the simulated pore solutions was investigated. Results showed that at a given pH (about 9.5) the corrosion susceptibility of Zn depends on anions concentration (carbonate and bicarbonate). Results obtained in simulated carbonated concrete Pore solutions showed that with low anion concentration Zn did not passivate while in presence of high levels of carbonate and bicarbonate the corrosion resistance is improved. Besides, the presence of chloride increased the corrosion susceptibility.

The corrosion inhibition behavior of Neem (*Azadirachta indica*) nature leaves extract as a green inhibitor of zinc corrosion in 2.0N hydrochloric acid (HCl) solutions has been studied using gravimetric and thermometric techniques for experiments conducted at 30 °C and 60 °C [53]. The results revealed that different concentrations of the *Azadirachta indica* (AZI) extract inhibit zinc corrosion and that inhibition efficiency of the extract varies with concentration and temperature. For extract concentrations studied and ranging from 9.09–23.08 mg / L, the maximum inhibition efficiency was 78.33% and 68.95% both at 23.08 mg / L AZI at 30 °C and 60 °C, respectively.

Introduction

The corrosion inhibition properties of *Ocimum tenuiflorum* (*Tulsi*) leaves extract as a potential green inhibitor of zinc corrosion in H_2SO_4 have been investigated using gravimetric and thermometric techniques [54]. The results show that different concentrations of the *Tulsi* extract have inhibited zinc corrosion and that the inhibition efficiency had varied with the concentration of extract and temperature of experimental corrosion half-cell.

The effect of sodium eperuate prepared from *Wallaba* (*Eperua falcata Aubl*) extract on zinc corrosion was investigated in alkaline solutions with chloride ions (i.e., simulated concrete pore solutions) by using electrochemical techniques [55]. Sodium eperuate inhibits the corrosion of zinc in 0.1 M NaCl solutions with pH 9.6. As its concentration increases to 1 g/L, the inhibition efficiency reaches approximately 92 %. In alkaline solutions with pH 12.6, sodium eperuate has no adverse effect on passivity of zinc, and retards the chloride attack. These suggest that sodium eperuate is an effective inhibitor for the protection of zinc in alkaline environments.

The aqueous extract of the leaves of henna (*lawsonia*) is tested as corrosion inhibitor of C-steel, nickel and zinc in acidic , neutral and alkaline solutions, using the polarization technique [56]. It was found that the extract acts as a good corrosion inhibitor for the three tested electrodes in all tested media. The inhibition efficiency increases as the added concentration of extract is increased. The degree of inhibition depends on the nature of metal and the type of the medium. For C-steel and nickel, the inhibition efficiency increases in the order: alkaline < neutral < acid, while in the case of zinc it increases in the order: acid < alkaline < neutral. The extract acts as a mixed inhibitor. The inhibitive action of the extract is discussed in view of adsorption of lawsonia molecules on the metal surface. It was found that this adsorption follows Langmuir adsorption isotherm in all tested systems.

Introduction

The formation of complex between metal cations and lawsone is also proposed as additional inhibition mechanism of C-steel and nickel corrosion.

The inhibition of the corrosion of zinc by acetone extract of *red onion* skin in hydrochloric acid solutions has been studied using weight loss method [57]. The results of the study reveal that different concentrations of the extract inhibit zinc corrosion. Inhibition efficiency of the extract is found to vary with concentration and temperature. The active component in red onion skin is quercetin. Acetone extract of red onion skin could serve as an effective and non-toxic inhibitor of the corrosion of zinc in hydrochloric acid solution.

The inhibitive effect of *fenugreek* (*Trigonella foenum graecum*) seeds extract on the corrosion of zinc in aqueous solution of 0.5 M sulphuric acid were investigated at 30,35,40, and 45 °C by potentiodynamic polarization and electrochemical impedance spectroscopy (EIS) techniques [58]. Potentiodynamic polarization curves indicated that the fenugreek seeds extract behaves as an anodic type inhibitor. EIS measurements showed that the dissolution process occurs under activation control. Inhibition was found to increase with increasing concentration of the fenugreek seeds extract but decreased with the increase of the temperature. The associated activation parameters were determined. Results showed that the *fenugreek* seeds extract could be used as an effective inhibitor for the corrosion of zinc in sulphuric acid media at higher temperature .

The effect of the extract of Aloe vera leaves on the corrosion of zinc in 2 M HCl solution was studied using weight loss technique [59]. A vera extract inhibited the corrosion of zinc in 2 M HCl solution and the

Introduction

inhibition efficiency increased with increasing concentration of the extract but decreased with increasing temperature. The adsorption of the inhibitor molecules on zinc surface was in accordance with Langmuir adsorption isotherm. A first-order kinetics relationship with respect to zinc was obtained with and without the extract from the kinetics treatment of the data.

The efficiency of some substituted N-arylpyrroles as zinc corrosion inhibitors in hydrochloric acid was examined by electrochemical (d.c. and a.c.) and gravimetric methods [60]. The influence of the structure and composition of a molecule on the inhibition characteristics was observed by investigation of the action of the functional group located on the pyrrole ring (-CHO) and at the ortho position of the benzene ring (-H, -Cl, -CH₃). The results have shown that all the organic compounds investigated possess good inhibiting properties. In contrast to most commercial acid corrosion inhibitors, which are highly toxic and very hazardous products, substituted N-arylpyrroles are nontoxic compounds with good environmental characteristics.

The effect of some amidopolyethylamine, with different numbers of ethylamine units on the corrosion of zinc electrode in ZnCl₂, NH₄Cl and (ZnCl₂ + NH₄Cl) electrolytes had been studied using galvanostatic polarization measurements [61]. The inhibition efficiency was found to increase with increasing concentration, number of ethylamine units per molecule and with decreasing the temperature. Inhibition was explained on the basis of adsorption of amidopolyethylamine molecules on the zinc electrode surface through their ethylamine groups. The inhibitors are adsorbed on the zinc electrode surface according to Langmuir adsorption isotherm. Some thermodynamic parameters are calculated and explained for the tested systems from the obtained data at different temperatures.

Introduction

The corrosion behavior of zinc electrode in ($\text{HNO}_3 + \text{HCl}$) binary acid mixture containing ethylamines was investigated [62]. In binary acid mixture, the corrosion rate increased with concentration of mixture acid and with the temperature. At constant mixture acid concentration, the inhibition efficiencies of ethylamines increase with the inhibitor concentration. Similarly, at constant inhibitor concentration, the inhibition efficiency increases with the increase in concentration of mixture acid. At IE % inhibitor concentration in (0.01 N $\text{HNO}_3 + 0.01$ N HCl) acid mixture at 301 K for 24 hr immersion period, the inhibition efficiency decreases in the order: ethylamine (98%) > diethylamide (95%) > triethylamine (91%). As temperature increases, the value of free energy ΔG^* increased, while percentage of inhibition decreases. The mode of inhibitor action appeared to be chemisorption since the plot of $\log (\theta/1-\theta)$ versus $\log C$ gave a straight line which suggests that the inhibitors cover both the anodic and cathodic regions through general adsorption following the Langmuir isotherm. Anodic and cathodic galvanostatic polarization curves showed little anodic but significant cathodic polarization.

The evaluation of Schiff bases derived from o-, m- and p-amino phenols and salicylaldehyde as corrosion inhibitors of zinc in sulfuric acid and to study their inhibitor mechanism [63]. The effect of various parameters on the behavior of these inhibitors has been studied using the weight loss and polarization measurements. In general, the ortho isomer was highly effective as a corrosion inhibitor because it forms a chelate with a six-membered ring and moreover the ortho isomer possessed pronounced electromeric effect. These inhibitors obey the Langmuir adsorption isotherm. The almost constant performance with temperature in the case of ortho and para isomers in 0.5M sulfuric acid suggested strong adsorption bonds. The thermodynamic parameters suggested that this strong interaction of the inhibitor molecules with the metal surface resulted in spontaneous adsorption. It may be concluded that a good

inhibitor is characterized by a relatively greater decrease in free energy of adsorption, lower entropy of adsorption and higher heat of adsorption. Polarization data indicated that all these isomers were predominantly cathodic inhibitors. The conjoint effect of external cathodic current and these inhibitors was either synergistic or additive.

The anodic behavior of Zn electrode in 1×10^{-2} M $\text{Na}_2\text{B}_4\text{O}_7$ solutions in the absence and presence of various concentrations of Na_2SO_4 , $\text{Na}_2\text{S}_2\text{O}_3$ or Na_2S as aggressive agent was studied by galvanostatic polarization technique [64]. In the absence of sulphur-containing anions in solution, the polarization curves are characterized by one distinct arrest corresponding to $\text{Zn}(\text{OH})_2$ and/or ZnO , after which the potential increased linearly with time due to the formation of barrier oxide film before reaching the oxygen evolution reaction. The duration time of the arrest decreased with increasing current density while the rate of oxide film formation increases. On the other hand, the duration time of the arrest increases with the number of anodic cyclization while the rate of oxide film formation decreased. Additions of low concentration of the aggressive anions have no effect on the passive film formed on the metal surface. The potential starts to oscillate within the oxygen evolution region with increases in the concentration of these aggressive anions. Further increases in the concentration of these aggressive anions are associated with impaired Zn passivity that might indicate pitting attack. The aggressiveness of the sulphur species decreases in the order: $\text{SO}_4^{2-} > \text{S}_2\text{O}_3^{2-} > \text{S}^{2-}$. The effect of raising pH of the solution on the anodic behavior of Zn electrode in the presence of SO_4^{2-} anions was also investigated. It was found that the raising the pH of the solution affecting on the rate of oxide film formation and the breakdown potential value.

The inhibiting effect of azithromycin toward the corrosion of zinc in various concentrations (0.01 to 0.05 M) of H_2SO_4 was studied using weight loss and hydrogen evolution methods of monitoring corrosion [65] .The results revealed that various concentrations of azithromycin (0.0001 to 0.0005 M) inhibited the corrosion of zinc in H_2SO_4 at different temperatures (303 to 333 K). The concentration of H_2SO_4 did not exert significant impact on the inhibition efficiency of azithromycin, but inhibition efficiencies were found to decrease with increase in the concentration of the inhibitor. Values of inhibition efficiency obtained from the weight loss measurements correlated strongly with those obtained from the hydrogen evolution measurements. The activation energies for the corrosion of zinc inhibited by azithromycin were higher than the values obtained for the blank. Thermodynamic data revealed that the adsorption of azithromycin on the surface of zinc was endothermic, spontaneous and was consistent with the adsorption model of Langmuir.

Chromates conversion coatings provide very effective corrosion protection for many metals. However, the high toxicity of chromate leads to an increasing interest in using non-toxic alternatives such as molybdates, silicates, rare earth metal ions and etc. In this work, quartz crystal microbalance (QCM) was applied as an in-situ technique to follow the film formation process on zinc (plated on gold) in acidic solutions containing an inorganic inhibitors, e.g. potassium chromate, sodium silicate, sodium molybdate or cerium nitrate [66]. Using an equation derived in this work, the interfacial mass change during the film formation process under different conditions was calculated, indicating three different film formation mechanisms. In the presence of K_2CrO_4 or Na_2SiO_3 , the film growth follows a mix-parabolic law, showing a process controlled by both ion diffusion and surface reaction. The apparent kinetic equations are $0.4t = -17.4 + 20\Delta m_f + (\Delta m_f)^2$ and $0.1t = 19.0 + 8.4\Delta m_f + 10(\Delta m_f)^2$ respectively (t and Δm are in seconds and $\mu\text{g}/\text{cm}^2$). In solutions

containing Na_2MoO_4 , a logarithmic law of $\Delta m_f = -24.7 + 6.6 \ln t$ was observed. Changing the inhibitor to $\text{Ce}(\text{NO}_3)_3$, the film growth was found to obey an asymptote law that could be fit into the equation of $\Delta m_f = 55.1(1 - \exp(-2.6 \times 10^{-3}t))$.

The inhibiting effect of cetylpyridinium bromide (CPB) toward corrosion of zinc in hydrochloric acid was investigated using weight loss method [67]. Experiments show that the adsorption of CPB on zinc is the key to inhibition, and the Langmuir isotherm is followed. Some important thermodynamic parameters in adsorption process were calculated from testing data by Sekine method.

In order to study the alkyl benzene sulfonate anion surfactant's corrosion inhibition and adsorption for the zinc in nitric acid, the corrosion inhibition of sodium do decylbenzene sulfonate on zinc in 3% nitric acid was Investigated with different temperatures and different concentration of sodium do decylbenzene sulfonate by weight-loss method [68]. Results showed that sodium do decylbenzene sulfonate had efficiently inhibited the corrosion of zinc .After its content achieved the certain concentration, the corrosion inhibition is in gross invariable. It was found that the adsorption of sodium do decylbenzene sulfonate on the surface of zinc is the important reason resulted from corrosion inhibition and that the rule of adsorption conforms to Langmuir's isotherm in 0~300 mg/L concentration. The experimental data were treated with Sekine method. Some thermodynamic parameters ,such as ΔH^0 , ΔS^0 and ΔG^0 are obtained.

Quantum chemical methods are particularly significant in the study of electrochemistry and provide researchers with a relatively quick way of studying the structure and behavior of corrosion inhibitors [69]. The originality of this review article is based on the fact that it is the first and unique general reference

for all those interested in the use of quantum chemical methods in corrosion inhibitor studies.

The inhibition effect of ethoxylated fatty acids were used as inhibitors for the corrosion of zinc metal in 1.0 M hydrochloric and 1.0 M sulfuric acid solutions at various temperatures ranging from 25 to 55 °C was investigated by weight loss and electrochemical methods [70]. The protection efficiency depends upon the type and concentration of the inhibitor and the nature of the acid medium. In both acid solutions the protection efficiencies of the inhibitors decrease with the increase in temperature. The inhibition was assumed to occur via the adsorption of the fatty acid molecules on the metal surface. The thermodynamic functions of dissolution and adsorption processes were calculated and discussed.

The passivation and pitting corrosion behavior of a zinc electrode in aerated neutral sodium nitrate solutions was investigated by cyclic voltammetry and chronopotentiometry techniques, complemented by exsitu scanning electron microscopy (SEM), X-ray diffraction (XRD) and energy dispersive X-ray (EDX) examinations of the electrode surface [71]. The potentiodynamic anodic polarization curves do not exhibit active dissolution region due to spontaneous passivation. The passivity is due to the presence of thin film of ZnO on the anode surface. The passive region is followed by pitting corrosion as a result of breakdown of the passive film. SEM images confirmed the existence of pits on the electrode surface. The breakdown potential decreased with an increase in NO_3^- concentration and temperature, but increased with increasing potential scan rate. Addition of SO_4^{2-} ions to the nitrate solution accelerates pitting corrosion, while addition of WO_4^{2-} and MoO_4^{2-} ions inhibits pitting corrosion. The chronopotentiometry measurements show that the incubation time for pitting initiation decreased with increase of NO_3^- concentration, temperature

and applied anodic current density. Addition of SO_4^{2-} ions decreased the rate of passive film growth and the incubation time, while the reverse changes produced by addition of either WO_4^{2-} or MoO_4^{2-} ions.

The inhibition of corrosion of zinc in 1.5M nitric acid, by some mono saccharides (glucose, fructose, mannose and galactose) in the concentration rang 5×10^{-2} to 3×10^{-1} M had been studied with respect to concentration of inhibitor and period of immersion [72]. In general, the inhibitor efficiency increased with the increase of the concentration of inhibitor due to the adsorption of these compounds on the zinc surface.

Tertiary arsines such as diphenylethylarsine (DPEA), diphenylmethyl arsine (DPMA), diphenyl arsine (TPA) have been used as Zn inhibitors for corrosion of zinc in perchloric acid solution [73]. These inhibitors inhibit corrosion effectively even in traces. The percentage inhibitor efficiency of the inhibitors are in the order $\text{DPEA} > \text{DPMA} > \text{TPA}$. The effect of pH and temperature on the inhibitor efficiency is studied. Steady state anodic and cathodic polarization data reveal that tertiary arsines act as interfacial corrosion inhibitors for zinc in acidic solution. The apparent free energies of adsorption of inhibitors have been reported for different possible modes of adsorption.

The corrosion of zinc in aqueous methanolic solution containing tri chloroacetic acid was studied [74]. Results indicated that the rate determining step in the corrosion was likely to be diffusion and /or adsorption of the participating species. The corrosion process of Zn was partly inhibited by the blockage of the surface by the adsorbed MeOH molecules.

The initial stage of atmospheric zinc corrosion using exsitu electrochemical impedance spectroscopy (EIS) in methanol electrolyte [75]. Compared with the traditional techniques for studying atmospheric corrosion,

such as gravimetry, the EIS technique significantly reduced the exposure time for detectable corrosion at any relative humidity from several days to a few hours. The samples were first exposed to synthetic atmospheres with careful control of O₂ and CO₂ concentrations, relative humidity and temperature. EIS was then used to measure the polarization resistance (R_p) of the exposed samples. The corrosion products were analyzed by a combination of grazing-angle X-ray diffraction, Fourier transform infrared spectroscopy and photoelectron spectroscopy. Several interesting phenomena occurring in the initial stage of corrosion were demonstrated by studying the electrochemical properties of the surface layer formed on the zinc. At high values of relative humidity (RH 95-100%) with CO₂ >40 ppm, the R_p of the surface film formed increased monotonically with time and relative humidity. At intermediate values of relative humidity (RH 50-85%) in the presence CO₂ (40-500ppm), R_p first increased with time, reached a maximum, and then fell from the maximum value before again rising slowly.

The inhibition of zinc corrosion by various triazole derivatives was investigated with respect to dependence on pH, potential E, inhibitor concentration $C_{inh.}$, zinc ion concentration C_{zn}^{2+} and exposure time t. current-Potential curves and measurements of weight loss showed that 3-amino-5-heptyl-1,2,4-triazole (AHT) is an excellent inhibitor of zinc corrosion in acid and weak alkaline solutions, while bisaminotriazole (BAT4 gives the best inhibition efficiency especially at pH 9 and low inhibitor concentration) [76]. Capacity potential curves and XPS-measurements show the formation of protective triazole layers with a maximum thickness of about 3nm. The chemical analysis of insoluble zinc triazole complexes precipitated in solution yields a stoichiometric ratio of Zn^{2+} and the triazole ring of 1:2. The presence of zinc triazole complex on the zinc surface is shown by XPS spectroscopy. The solubility, adsorbability and hydrophobicity of the triazole molecules and the

stability of the zinc-triazole complexes are found to be the most important factors influencing the inhibition efficiency of the triazole derivatives under varying condition.

The effect of quinoline, benzo (f) quinoline and 8-hydroxyquinoline on the electrochemical and corrosion behavior of zinc, Zn 2% Cd and Zn 2% Pb alloys in deaerated 0.1 M HCl solution was studied using the potentiostatic technique [77]. Although quinoline inhibited the corrosion of zinc at all examined concentrations, it accelerated the corrosion of the alloys. As an inhibitor, quinoline was found to have a predominant anodic effect and its adsorption conformed to the Temkin isotherm at concentrations $>10^{-4}\text{M}$, benzo (f) quinoline inhibited the corrosion of both zinc and the alloys. Inhibition was found to be predominantly anodic without changing the mechanism of zinc dissolution, inhibition by 8-hydroxyquinoline was found to be purely anodic occurring by surface chelation, resulting in a change of the mechanism of zinc dissolution.

The corrosion behavior of zinc in stagnant distilled water containing 0-70 percent (v/v) methanol, ethanol or n-propanol was investigated at 25 - 40 °C using potentiodynamic polarization technique [78]. The activation parameters that govern zinc corrosion in mixed solvent system were also calculated. The data revealed that, the corrosion of zinc in mixed solvents depends on two factors : the hydrolysis rates of the metals ions in alcohol-water solutions and the chemisorption of organic solvent molecules at the metal surface .When the later effect predominant the final result is an increase of the inhibiting effect. On the other hand, when the first factor is dominant the final result is a decrease in the protection efficiency and may exhibit an accelerating effect. Special attention should be made on using mixed water-alcohol solvents, 50 percent (v/v) has unexpected accelerating effect. Whereas 70 percent (v/v) exhibits

protection efficiency of ≈ 58 percent. Owing environmental concerns, the use of alcohol in automotive fuel increases. Therefore, it is of importance to study the corrosion behavior of zinc in alcoholic solution.

Rangel *et al* [79] studied the corrosion and inhibition corrosion of zinc by polyphosphate, using electrochemical impedance spectroscopy (EIS) and cyclic voltammetry artificial waters as electrolytes. The anodic dissolution reaction inhibited mixed kinetics, which changed to diffusion control when calcium ions were removed. The effect of calcium to polyphosphate ratio on the corrosion rate of zinc was studied to determine the composition, which gave the optimum protection.

The corrosion and electrochemical properties of three zinc single crystal surfaces with different orientations had been investigated [80]. In near-neutral 1 M $(\text{NH}_4)_2\text{SO}_4$, the corrosion rates on all three surfaces were found to be similar. However, the SEM morphologies of the corresponding corroded surfaces were markedly different from each other, but consistent with preferential attack of $\{11\bar{2}0\}$ surfaces. In alkaline 0.5 N NaOH solution, the three sample orientations showed significantly different reactivities, with the $(11\bar{2}0)$ surface exhibiting the highest reactivity and corrosion rate. Here, passivation ultimately occurred and the difference in the corrosion performance of the three surfaces, even for small over voltages, is attributed to the presence of oxide or hydrated oxide films.

Quantum mechanical calculations have been applied to a series of pyrazole derivatives used as corrosion inhibitors for zinc, copper and α - brass in order to assess quantum chemistry as means of evaluating effectiveness of corrosion inhibitors [81]. The corresponding structures have been optimized the energies and coefficients of their molecular orbitals (HOMO and LUMO) have been computed using the semi empirical method, MNDO. The theoretical

results are then compared with experimental data. The inhibition action occurs via chelation of the active centres with the metal surface. The position of the substituent group with respect to the pyrazole ring also affects the inhibition efficiency of the inhibitor molecules [82].

The influence of benzotriazole (BTA) on the corrosion of pure zinc in $1\text{NH}_2\text{SO}_4$ has been studied by weight loss method[83]. The additive concentrations in the range of 10^{-5}M to 10^{-1}M were examined at four different temperatures. The heat of adsorption and the activation energy were calculated for the corrosion inhibition process. Finally, free energy change for the corrosion inhibition process had been found out. It was, observed that benzotriazole acted as a good inhibitor for the corrosion of zinc at low temperatures. At higher temperatures the inhibition efficiency decreased considerably.

The corrosion of zinc in ammonium chloride, both pure and containing various organic compounds, has been studied by means of analytical and electrochemical methods as determination of the zinc dissolved and the hydrogen evolved, I-V curve recording and impedance measurements [84]. The obtained results in a potential region near the zinc corrosion potential showed that the cathodic reaction of hydrogen discharge does not fit a simple exponential law because the Tafel coefficient appears to be electrode potential dependent. The experimental findings proved that only five of the 25 organic substances tested were found to behave as zinc corrosion inhibitors in decreasing order of influence.

Impedance diagrams for protected and non-protected zinc were recorded in chloride solutions using stationary and rotating disk electrodes [85]. Some of the determined impedance parameters can be very useful in the characterization of the processes of corrosion protection and diffusion.

Pitting corrosion of zinc in neutral inhibited conditions was studied [86]. The effect on addition of aggressive salts such as LiCl, NaCl, RbCl and MgCl₂ on the steady-state potential of zinc electrode previously equilibrated in passivating chromate solution was established. S-shaped curves were obtained for the variation of the steady state potential with good environmental characteristics. The quantity of aggressive salt added for each inhibitor concentration, the addition of aggressive ions up to a certain concentration has no effect on the passivity of zinc. However, Cl⁻ ion concentration caused destruction of the passive film and initiation of pitting corrosion. Destruction of passivity occurred after an induction period, which decreases with the increase in the concentration of the attacking ion or the decrease in that of the inhibiting ions. The efficiency of these salts in initiating pitting corrosion increased in the order: RbCl < MgCl₂ < KCl < NaCl < LiCl. The change in the degree of aggressiveness of these salts could be attributed either to the incorporation of the cations in the passive film or to their effect on pH.

The kinetic of corrosion of pure zinc in trichloroacetic (TCA) was investigated over a wide range of solvent compositions and temperatures [87]. The variation of thermodynamic properties of the activated complex with the mole fraction of methanol revealed the existence of preferential solvation. The determined isokinetic temperature indicated that the reaction was enthalpy controlled where the interaction between methanol and zinc surface played an important role.

The electrochemical behavior of zinc in NaOH solutions was investigated by using potentiodynamic technique and complemented by X-ray analysis [88]. The E/I curve exhibit active, passive and transpassive regions prior to oxygen evolution. The active region displays two anodic peaks. The passivity due to the formation of a compact Zn(OH)₂ film on the anode

surface. The transpassive region is assigned to the electro formation of ZnO. The reverse sweep shows an activation anodic peak and one cathodic peak prior to hydrogen evolution. The influence of increasing additives of NaCl, NaBr and NaI on the anodic behavior of zinc in NaOH solutions has been studied. The halides stimulate the active dissolution of zinc and tend to break down the passive film, leading to pitting corrosion. The aggressiveness of the halide anions towards the stability of the passive film decreases in the order: $I^- > Br^- > Cl^-$. The susceptibility of zinc anode to pitting corrosion enhances with increasing the halide ion concentration but decreases with increasing both the alkali concentration and the sweep rate.

Inhibiting effect of semicarbazide, thiosemicarbazide, sym diphenylcarbazon towards corrosion of zinc in hydrochloric acid had been investigated [89]. The rate of corrosion depended on the nature of the inhibitor and its concentration. The values of inhibition efficiency from, weight-loss thermometric measurements were in good agreement with those obtained from polarization studies. The inhibitors used acted as mixed adsorption type inhibitors. Increased adsorption resulting from an increase in the electron density at the reactive C=S, C=O groups and N-atoms. The thermodynamic parameters of adsorption obtained using Bockris-Swinkels adsorption isotherm revealed a strong interaction of these carbazide on zinc surface.

The inhibiting effect of p-chlorobenzylidencyanothioacetamide towards corrosion of zinc in 1N HCl using three different techniques e.g.(weight loss, volume of hydrogen evolution and polarization measurements) [90]. All the results of the three methods were in good agreement that the inhibitor efficiency increased with increase of inhibitor concentrations. The degree of surface coverage varied linearly with logarithm of inhibitor concentration fitting Temkin isotherm. The inhibitor molecules were physically adsorbed on the zinc surface

as indicated from the decrease in the inhibitor efficiency with the rise of temperature.

The corrosion behavior of electrodeposited zinc and Zn-Ni alloy in synthetic sea water with and without sulphide present as a pollutant was studied [91]. Zinc undergoes galvanic dissolution giving rise the corrosion products consisting mainly of zinc oxide and hydroxide. Unless these products form a compact layer, atmospheric oxygen will have easy access to the steel surface and the corrosion of zinc will be accelerated.

The anodic behavior of Zn in 0.1 M NaOH containing various concentrations of Na_2SO_4 , Na_2SO_3 , Na_2S , $\text{Na}_2\text{S}_2\text{O}_3$ or NH_4SCN was studied by means of the potentiodynamic technique, complemented by X-ray diffraction analysis and scanning electron microscopy [92]. In the absence of sulphur-containing anions in solution, the cyclic voltammogram displays two anodic peaks in the forward scan prior to reaching the oxygen evolution potential. The first anodic peak A_1 is related to the electro formation of $\text{Zn}(\text{OH})_2$, while the more positive peak A_2 is assigned to the formation of ZnO_2 . The reverse scan exhibits a reactivated anodic peak A_3 and one cathodic peak $C1$, prior to reaching the hydrogen evolution potential. The presence of either SO_4^{2-} or SO_3^{2-} Stimulates the active dissolution of Zn while the presence of S^{2-} (and / or SH^-), $\text{S}_2\text{O}_3^{2-}$ or SCN^- inhibits it, presumably as a result of electro formation of sulphur-containing solid phases preceding the formation of $\text{Zn}(\text{OH})_2$. Also, the presence of one of the cited anions studied in the alkali solution produces pitting of Zn at a certain specific pitting potential. The existence of pitting is confirmed by scanning electron microscopy. The aggressiveness of the sulphur species decreases in the order $\text{SCN}^- > \text{SO}_4^{2-} > \text{SO}_3^{2-} > \text{S}_2\text{O}_3^{2-} > \text{S}^{2-}$. The pitting potential decreases with increasing concentration of the sulphur species.

The corrosion behavior of Zn and ZnO coatings in 3.5 % NaCl solution, with and without illumination, was investigated by weight loss and potentiodynamic anodic polarization measurements [93]. The ZnO films, of a range of thicknesses, were formed by anodizing in borate solution. In dark conditions, the corrosion rate was found to increase initially with increase in the oxide thickness, whereas above a certain thickness the corrosion rate decreased. These results are attributed to a thin layer of oxide with a non-uniform structure formed during times of 1–4 hr. anodizing, while for longer times of anodizing, a thicker oxide is formed. The corrosion products consist mainly of $\text{Zn}(\text{OH})_2$. Under illumination conditions, the corrosion rate decreased as the oxide thickness increased, due to an initial, more rapid formation of corrosion products than in the dark, which creates a protective layer, delaying further corrosion. The corrosion products consist mainly of zinc oxy chlorides, which have more protective properties than the $\text{Zn}(\text{OH})_2$. The presence of zinc oxychlorides in the corrosion products increases with time of anodizing. For thin films, corrosion rates were greater under illumination, but for thicker films, corrosion rates were greater in the dark. Uniform corrosion was observed in dark conditions, but under illumination, pitting corrosion occurred and higher current densities were observed than in the dark.

The inhibition corrosion processes of zinc using furfural as chemical inhibitor in ethanolic solutions was studied [94]. The results obtained from different electrochemical methods confirmed this effect that, inhibition depended upon the adsorption step and was affected by the incidence of polychromatic light on the metal surface. Protection efficiency of furfural was higher when the system was kept in the dark than when under illumination, An inhibition process involving and adsorption step of furfural was proposed.

Mlieller *et al* [95, 96] investigated the inhibition corrosion of zinc pigments in an aqueous alkaline paint medium by hydrogen evolution. The corrosion reaction was inhibited by addition of chelate form aromatic-hydroxyl compounds of low molecular weight. Propoctly, dodecygallate and low molecular weight. Styrene maliec acid and styrene-acrylic acid/styrene-acrylate copolymers were found to be good inhibitors for zinc pigments. Inhibition by oligomeric phenolic (resole) could be explained by a chelation reaction with zinc (II).

Zinc pigments react in aqueous alkaline media (e.g. water-borne paints) by the evolution of hydrogen. Heterocyclic compounds can inhibit this corrosion reaction [97]. The corrosion inhibiting effect of the heterocyclic depends strongly on the base which is used for adjusting the pH value to 10. Ammonia accelerates the corrosion reaction very much; the protection factors for the heterocyclic are 5–40%. The examined heterocyclic inhibit significantly better than dimethyl ethanolamine or sodium hydroxide are used as bases, protection factors increase up to 98%.

Zinc pigments react in aqueous alkaline media (e.g. water-borne paints) by the evolution of hydrogen [98]. This corrosion reaction can be inhibited at a pH value of 10 (DMEA) by the addition of amino methylene phosphonic acids, amphiphilic partial esters of phosphoric acid and phosphoric acid. The protection factors for the corrosion inhibition of zinc pigment (borderline Lewis acid) by salts of amino methylenephosphonic acids and phosphoric acid (hard Lewis bases) are smaller for the corrosion inhibition of aluminum pigments (hard Lewis acid).

Zinc pigments react in aqueous alkaline media (e.g. water-borne paints) by the evolution of hydrogen which can be measured gas volumetrically [99]. The addition of both pure citric acid and pure metal salts stimulated the

Introduction

corrosion reaction of zinc pigment in aqueous alkaline media. The addition of soluble zinc (II) and aluminum(III) chelates of citric acid reduced the hydrogen evolution of zinc pigment dispersions compared to pure citric acid; but the level of hydrogen evolved was still very high. In contrast, soluble cerium(III) chelates of citric acid were powerful corrosion inhibitors for zinc pigments in aqueous alkaline media. The pronounced corrosion inhibiting effect of the cerium(III) chelates could be attributed to cerium and not to the charge of the chelates.

The rate of corrosion of electroplated zinc in near-neutral chloride solutions can be lowered by as much as 75% by adding fine, inert particles of substances such as MnO_2 , Fe_3O_4 , SiC and TiN to the well-stirred solution [100]. Spreading of local areas of etching is also stopped.

Corrosion studied showed normal dodecylamine (NDDA) to be effective as anodic inhibitor for zinc corrosion in ammonium chloride media [101]. The inhibiting effect was found to be associated with adsorption on active centers of the zinc surface. The adsorption was potential dependent and the inhibiting effect diminished with positive shift of the zinc electrode during discharge. This feature makes it possible for NDDA to be used in zinc-manganese dry batteries as a substitute for the environmentally harmful mercury inhibitor.

Pourbaix diagrams (potential / pH diagrams) for zinc at 25–300 °C was revised [102]. The diagrams were calculated for three concentrations, 10^{-5} , 10^{-6} and 10^{-8} ml^{-1} , the latter for use in high purity water such as in nuclear power reactors. Extrapolation of the electrochemical data to elevated temperatures was performed with the revised model of Helgeson-Kirkham-Flowers, which also allows uncharged aqueous complexes, such as

$\text{Zn}(\text{OH})_{2(\text{aq})}$, to be handled. The calculations show that the hydroxide of zinc does not passivate at the concentration of 10^{-6} M, due to the uncharged zinc (II) complex, $\text{Zn}(\text{OH})_{2(\text{aq})}$. However, at concentrations $\geq 10^{-5.7}$ ml^{-1} zinc passivates by formation of ZnO , which is stable in the temperature interval investigated.

The corrosion of Zn in both aerated by air ($\text{O}_2 + \text{N}_2$), and deaerated by N_2 , solutions of KNO_3 at concentrations largely varying, 10^{-5} to 1 M, was studied [103]. The corrosion process is followed in time by potentiometry and the potential of Zn electrode (vs. SCE) vs. time plots is derived. In both cases, a transition period is observed until a steady state is achieved where the rate of Zn^{2+} and OH^- production becomes equal to the rate of $\text{Zn}(\text{OH})_2$ precipitate formation. In the aerated solutions the potential and corrosion rate decrease with time while in the de-aerated solutions they pass successively through a minimum and a maximum before a steady state is achieved. By a suitable potentiometric analysis the results are explained. The most important factors found to be affecting the mechanism of corrosion process are presented. From the discovery of the mechanism and the factors affecting the Zn corrosion, predictions for promoting or slowing down the corrosion may be derived.

The corrosion behavior of zinc and its alloys in H_2SO_4 solutions with oxygen and ferric ions was studied using a potentiostatic polarization [104]. Cathodic reduction of oxygen mainly was controlled by chemical reaction and that of Fe^{3+} ions was controlled by diffusion. The overall cathodic process was the summation of the reduction of oxygen and Fe^{3+} ions, corrosion of zinc controlled mainly by reduction of water. Benzotriazole (BTAH) was used as corrosion inhibitor for dissolution of zinc in 1M H_2SO_4 investigated in aerated and deaerated solutions. BTAH was found to be a useful inhibitor, and the inhibition layer was shown to be stable and

persistent. By scanning electron microscopy (SEM) the surface of zinc after corrosion in the presence and absence of BTAH was examined that the inhibiting effect of BTAH towards the corrosion of zinc is due to formation of a protective film.

The inhibiting properties of some organic phosphonium and ammonium compounds were studied with respect to the corrosion of zinc in 1M H_3PO_4 solution [105]. It was found that onium compounds which have π -electron system are adsorbed following Frumkin's adsorption isotherm and provide better inhibition efficiency than those containing no electron system. The adsorption of the latter compounds was found to obey Langmuir's isotherm. Both potentiostatic and electrochemical impedance techniques proved that the studied onium compounds act as primary interface inhibitors without changing the mechanism of either hydrogen evolution reaction or zinc dissolution.

The corrosion behavior of zinc metal in some organic solvents was tested electrochemically using galvanometric polarization measurements [106]. Results showed that the studied organic solvents act as mixed type inhibitors. The inhibition was assumed to occur via physical adsorption of the inhibitor molecules, fitting a Temkin's isotherm. The inhibition efficiency of the solvents increase in the order: glycerol > ethyleneglycol > DMSO > dioxane. This order is not affected by the variation in temperature in the range 35-55°C. The increase in temperature was found to increase the corrosion in absence and presence of inhibitors. Some thermodynamic parameters for adsorption were also computed and discussed.

The effect of a new organic molecule with chelating groups on the corrosion behavior of zinc was investigated [107]. Electrochemical studies of the zinc specimens were performed in aerated aqueous solution (0.2M

Na_2SO_4 + 0.2M NaCl, pH 6) by means of electrochemical impedance spectroscopy (EIS), as well as polarization curves using a rotating disk electrode. The treatment was achieved by immersion in solutions of variable concentration of the organic molecule and for different immersion times. The influence of the treatment bath temperature was also studied. The recorded electrochemical data showed that the corrosion resistance of the treated samples was greatly enhanced when compared to the untreated zinc. Moreover, the treatment induced a basic modification of the cathodic corrosion behavior of zinc decreasing the electron transfer rate. The corrosion inhibition could be explained by a chelation reaction between zinc and organic molecule and the formation of a protective organometallic layer on the metal surface. Fourier Transform Infrared Spectroscopy (FT-IR) was applied in order to investigate this layer.

The anodic behavior of zinc in $\text{Na}_2\text{B}_4\text{O}_7$ solutions in the absence and presence of Cl^- anion as an aggressive anion has been investigated by the galvanostatic polarization technique [108]. In the absence of Cl^- anion, the polarization curves are characterized by one distinct arrest corresponding to $\text{Zn}(\text{OH})_2$ or ZnO after which the potential increases linearly with time before reaching the oxygen evolution region. Addition of low concentrations of Cl^- anions, has no effect on the passive film formed on the metal surface. The potential starts to oscillate within the oxygen evolution region with an increase in the concentration of the Cl^- anion. This suggests interference of Cl^- anion with oxygen evolution. Further increases in the concentration of Cl^- anions are associated with breakdown of Zn passivity, this denoting the destruction of the passivating film and initiation of pits. The susceptibility of zinc to pitting corrosion is enhanced with increasing Cl^- anion concentration but decreases with an increase of both the $\text{Na}_2\text{B}_4\text{O}_7$ concentration and current density. Addition of increasing concentrations of tungstate,

phosphate or molybdate anions causes a shift of the breakdown potential in the noble direction, indicating the inhibitive effect of the added anion on the pitting attack. In contrast, addition of the sulphate anion enhances the pitting attack.

The pitting corrosion behavior of Zn in neutral (pH 6.8) Na_2SO_4 solutions was studied by using potentiodynamic and cyclic voltammetry techniques and complemented by X-ray analysis under the effect of electrolyte concentration, scan rate, temperature and pH[109]. The voltammograms involve active/passive transition prior to the initiation of pitting corrosion. The active region displays one anodic peak. The passivity is due to the formation of ZnO film on the anode surface. The critical pitting potential decreases with increasing sulphate ion concentration and temperature but decreases with scan rate. Increasing the acidity or alkalinity of the medium enhances the pitting corrosion. The effects of adding increasing concentrations of $\text{Cr}_2\text{O}_4^{2-}$, $\text{Cr}_2\text{O}_7^{2-}$, WO_4^{2-} , MoO_4^{2-} and NO_2^- anions on sulphate pitting corrosion of Zn were investigated. These anions inhibit the active dissolution and pitting corrosion and the extent of inhibition depends upon the type and concentration of the inhibitors. The adsorption characteristics of these anions on the electrode surface play a significant role in inhibition.

Using a simple model cell the susceptibility of the zinc electrode to pitting corrosion by SO_4^{2-} , SO_3^{2-} , $\text{S}_2\text{O}_3^{2-}$ and S^{2-} anions were examined in naturally aerated carbonate solutions[110]. It was found that, pitting started after an induction period π , which depended on the type and concentration of the aggressive and passivating anions. The pitting corrosion current increased with time until steady state values were attained. These values depended on both the type and the concentration of the passivating and pitting anions. For the same concentration of the passivating anions, the corrosion current varied

Introduction

with the concentration of the aggressive anion according to the relation: $\log i_{\text{pit.}} = a_1 + b_1 \log C_{\text{agg.}}$. At a constant concentration of the aggressive anion, the corrosion current varied with the concentration of the passivating anions according to: $\log i_{\text{pit.}} = a_2 - b_2 \log C_{\text{pass.}}$. The constants a_1 (a_2) and b_1 (b_2) were determined for all the systems studied. From the values of a_1 the corrosivity of the sulphur-containing anions is found to decrease in the order $\text{SO}_4^{2-} > \text{SO}_3^{2-} > \text{S}_2\text{O}_3^{2-} > \text{S}^{2-}$.

The corrosion behavior of zinc deposits obtained under pulsed current electrodeposition from an acidic chloride bath in the presence and absence of coumarin has been investigated [111]. The effects of pulse peak current density (J_p) on the morphology of zinc deposits were studied by scanning electron microscopy. An increase in J_p from 40 to 280 A dm^{-2} yields deposits with a finer grain size. The refinement of the grain size was more considerable in the presence of coumarin ($J_p = 280 \text{ A dm}^{-2}$). The preferred orientation of zinc deposits was studied by X-ray diffraction. At $J_p = 40 \text{ A dm}^{-2}$, the preferred orientation of zinc deposits was (1 0 3) and changed to (0 0 2) at $J_p = 80 \text{ A dm}^{-2}$. An increase in J_p to 280 A dm^{-2} did not change the preferred crystallographic orientations except for an increase in the peak intensity of the (0 0 2) plane. In the presence of coumarin, the preferred crystallographic orientations changed at $J_p = 280 \text{ A dm}^{-2}$ from the (0 0 2) plane to the (1 0 3) plane. The corrosion behavior was investigated in an aerated 3.5% NaCl solution; the anodic polarization and electrochemical impedance spectroscopy curves were performed. The corrosion resistance of zinc deposits was improved by increasing the pulse peak current density (J_p); whereas, the presence of coumarin did not improve the corrosion resistance.

The performance of ethylene diamine, N, N'-dibenzylidene, ethylene diamine, N, N'-di (p-methoxybenzylid-ene), ethylenediamine N, N'-disalicylidene

Introduction

were used as corrosion inhibitors for zinc in sulphuric acid [112]. The effect of various parameters on the efficiency of these inhibitors had been studied. Ethylene diamine, N, N'-di (p- methoxy benzyldene) and ethylene diamine N, N'-di salicylidene give 99% protection under a variety of conditions. Activation energies in the presence and absence of inhibitors have been calculated. It appears that an efficient inhibitor is characterized by a relatively greater decrease in free energy of adsorption, relatively lower entropy of adsorption and relatively lower heat of adsorption. Galvanostatic polarization studies indicate that these are basically cathodic inhibitors. Cathodic protection in the presence of these inhibitors was studied. With an efficient inhibitor, cathodic protection was achieved at potentials much less negative than that required for plain acid. The difference between protective potential and corrosion potential appears to be less for an effective.

The inhibiting effect of 2-mercaptobenzothiazole (MBT) self-assembled monolayer on silver and zinc electrodes were comparatively studied [113] by means of electrochemical impedance spectroscopy (EIS). The adsorption geometries of MBT monolayer on zinc and silver electrodes were observed by surface enhanced Raman scattering (SERS) technique. The SERS spectra implied that monolayer of MBT could be self-assembled on Ag surface through S^{10} and N^3 atoms and the molecular plane should be tilted with respect to the surface. On Zn surface, MBT molecules formed monolayer via both S atoms the other moieties of the molecule away from the surface. From the insitu electrochemical SERS results it can be found that MBT monolayer on both Ag and Zn surfaces experienced the changes of adsorption fashions as the potential shifting to more negative direction.

The effect on the corrosion behavior of zinc of a new organic molecule with chelating groups was investigated [114]. Electrochemical studies of the

Introduction

zinc specimens were performed in aqueous sulfate–chloride solution (0.2 M Na_2SO_4 + 0.2 M NaCl, pH 5.6) using potentiostatic polarization techniques with a rotating disk electrode. Zinc samples, previously treated by immersion in the inhibiting organic solution, presented good corrosion resistance . The influence of the treatment bath pH and temperature on the protection efficiency has been emphasized. The recorded electrochemical data indicated a basic modification of the cathodic corrosion behavior of the treated zinc resulting in a decrease of the electron transferrate. Corrosion protection could be explained by a chelation reaction between zinc and organic molecules and the consequent growth of an organometallic layer strongly attached to the metal surface which prevented the formation of porous corrosion products in the chloride-sulfate medium. This protective film was studied using several surface analysis techniques such as X-ray photoelectron spectroscopy (XPS), scanning electron microscopy (SEM–EDS) and Fourier transform infrared spectroscopy (FTIR).

The corrosive behavior of zinc in HCl solution containing various concentrations of glutaraldehyde GTD, glycine GLN, methionine MTN, and their condensation products formed between GTD + GLN (CP1) and GTD + MTN (CP2) was investigated [115]. The corrosion-inhibitive action of these compounds on zinc metal was studied using chemical and electrochemical methods. The results showed that the compound CP_2 is the best inhibitor and that its inhibition efficiency reaches 92.56 % at 10^{-2} M in 0.05 M acid concentration. As an inhibitor, CP2 was found to have a predominant cathodic effect and its adsorption was confirmed with the Temkin isotherm. The effect of temperature on the corrosion of zinc was investigated by the weight-loss method. The morphology of the corroded surface was studied by SEM technique to obtain information about the adsorption of inhibitor molecules on the zinc surface.

Sulphur containing organic compounds decreased the corrosion rate by increasing the hydrogen over potential on zinc metal due to their electron donating groups. Their inhibiting effect was found to be associated with their adsorption on the active centers of the metal. The inhibition efficiencies of some aliphatic sulphide in ammonium chloride solution have been studied by weight loss studies, polarization and impedance measurements [116]. The effect of substituent groups is correlated with their inhibition performance. These studies due to their relevance in Zn Manganese dry batteries assume their importance.

The reaction of water based solution of 1,5-diphosphonopentane (DPP) with high purity polycrystalline zinc surface was investigated at room temperature [117] . XRD and XPS studies evidenced the formation of crystalline zinc –phosphonate film on the metal surface. The former layers give hydrophilic properties to the surface. A conversion-type interaction of diphosphonic acid compounds with the oxidized zinc surface was unambiguously shown by XPS analysis. Conclusive results were obtained by synthesized zinc-diphosphonate model compounds imitating the ones developed on the zinc surface, revealing a simple, closely 1:1 ratio of the phosphonate groups with zinc . Reactions with both diphosphonates resulted in significant protective effect of zinc against corrosion, although the structure and quality of the formed layers exhibit marked differences. The in-depth distribution of the composition and dissimilarity of the layer thickness were determined by glow discharge optical emission spectrometry. The corrosion inhibition was explained by the formation of insoluble zinc-phosphonate salt on the zinc surface, blocking the zinc dissolution process.

Quantum chemical methods are particularly significant in the study of electrochemistry and provide researchers with a relatively quick way of

Introduction

studying the structure and behavior of corrosion inhibitors[118]. The originality of this review is based on the fact that it is the first and unique general reference for all those interested in the use of quantum chemical methods in corrosion inhibitor studies. It begins with a concise summary of the most used quantum chemical parameters and methods.

The efficiency of various imidazole derivatives as zinc corrosion inhibitors in hydrochloric acid (HCl) was investigated using electrochemical and gravimetric methods[119]. A difference in efficiency (η) was observed with the introduction of different substituents into an imidazole skeleton. It was established that substituents which increased the electron density at the reaction center improved the corrosion inhibiting properties of the heterocyclic compound. A linear correlation between reaction kinetic data and the sum of the polar substituent constants was obtained.

The corrosion inhibition of zinc in 0.1M HCl in presence and absence of some hydrazide derivatives was investigated using mass-loss and polarization techniques[120]. The obtained results showed that the inhibition efficiency increased with the increase of the concentration of the additives and decreased with the increase of temperature. Synergism between I^- , SCN^- and Br^- anions and hydrazide derivatives was proposed. The polarization curves showed that hydrazide derivatives act as mixed-type inhibitors, acting predominantly as cathodic inhibitors for zinc in 0.1 M HCl. The adsorption of these hydrazide derivatives on zinc surface follows Temkin's adsorption isotherm. Some thermodynamic parameters were calculated. The kinetic parameters of corrosion of zinc in HCl solution have been studied.

Adsorption of the quaternary ammonium Gemini surfactants alkanediyl- α,ω -bis-(dimethyl dodecyl ammonium bromide), referred as $C_{12-s}-C_{12}\cdot 2Br$ ($s = 2,3,4,6$), on the zinc surface in 0.5 mol/L H_2SO_4 solution was investigated using gravimetric measurements [121]. The adsorption of $C_{12-s}-C_{12}\cdot 2Br$ on the zinc surface accorded to the Frumkin isotherm model. The maximal inhibition efficiency for zinc was reached at the saturated adsorption concentration C_c that was larger than its critical micelle concentration in 0.5 mol/L H_2SO_4 solution. The inhibition efficiency for zinc slightly reduced with increasing s since $C_{12-s}-C_{12}\cdot 2Br$ formed different morphologies of the surface aggregates. The adsorption ability and the inhibition efficiency for corrosion reduced with increment of temperature.

The pitting corrosion behavior of zinc in each of the following solutions NaCl, NaBr and NaI were studied by potentiodynamic and cyclic voltammetry techniques under the influence of different experimental variables [122]. In these solutions, the anodic sweep exhibits an active/passive transition prior to the initiation of pitting corrosion. The active dissolution region displays one anodic peak A_1 . Passivity is due to the existence of a protective film of ZnO on the anodic surface. At a certain specific potential, pitting potential, breakdown of the anodic passivity occurs caused by field-stimulating halide penetration into the passive oxide film at point defects. The aggressiveness of the halide ions towards the stability of the passive film decreases in the order: $Cl^- > Br^- > I^-$. The susceptibility of zinc to pitting corrosion enhances with increasing the halide ion concentration and the temperature but decreases with the sweep rate. The cathodic sweep shows two reduction peaks C_1 and C_2 . The more negative cathodic peak C_1 is a conjugate of the anodic peak A_1 while the cathodic peak C_2 is related to the electro reduction of the pitting corrosion

products. The existence of pitting corrosion was confirmed by scanning electron microscopy.

The use of potentiodynamic anodic polarization, cyclic voltammetry and chronoamperometry techniques in order to study the pitting corrosion susceptibility of a Zn electrode in KOH solutions containing KSCN as a pitting corrosion agent[123]. Results demonstrated that in the absence of KSCN, the anodic voltammetric response displays two anodic peaks prior to reaching the oxygen evolution potential. The first anodic peak A_1 is related to the electro formation of $Zn(OH)_2$. Peak A_1 is followed by a wide passive region which extends up to the appearance of the second anodic peak A_2 . The latter is assigned to the formation of ZnO_2 . Addition of SCN^- ions to the KOH solutions stimulates the anodic dissolution through peak A_1 and breaks down the passive layer prior to peak A_2 . The breakdown potential decreases with an increase in SCN^- concentration and temperature, but increases with an increase in KOH concentration and potential scan rate. Successive cycling leads to a progressive increase in breakdown potential. The current / time transients show that the incubation time for passivity breakdown decreases slightly with increasing applied positive potential, SCN^- concentration, and temperature.

The changes in the pitting corrosion current density with time on zinc electrode concerning the concentration of both the passivating borate and the aggressive chloride anions were followed using a simple electrolytic cell [124]. The pitting corrosion currents started to flow after an induction period, τ . This period is found to be a function of the concentration of Cl^- anion, according to the relation $\log \tau = \beta - \gamma \log C_{Cl^-}$. The pitting corrosion currents finally reached a steady-state value, which depended on the concentration of both $B_4O_7^{2-}$ and Cl^- anions. At a constant $B_4O_7^{2-}$ anion

concentration, the pitting corrosion current varied with the concentration of Cl^- anion according to the relation $\log i_{\text{pit}} = a_1 + b_1 \log C_{\text{Cl}^-}$. It also varied at constant Cl^- anion concentration and various $\text{B}_4\text{O}_7^{2-}$ anion concentration according to the relation $\log i_{\text{pit}} = a_2 - b_2 \log C_{\text{B}_4\text{O}_7^{2-}}$. The susceptibility of the passivating zinc to pitting corrosion was found to be increasing as the temperature and pH of the solution increased. Results are discussed on the basis of adsorption of the aggressive anion on the passivating film, followed by penetration through the film and incorporation in it. This undermines the oxide film and caused pitting corrosion.

The electrochemical frequency modulation (EFM) technique provided a new tool for electrochemical corrosion monitoring [125]. EFM is a non-destructive technique as electrochemical impedance spectroscopy (EIS). EFM technique was used in comparison with the traditional dc and ac techniques. Results obtained by EFM technique were shown to be in agreement with other electrochemical techniques. With EFM technique, a corrosion rate can be obtained instantaneously in very short time which makes this technique ideal in online corrosion monitoring. New synthesized thiourea derivative named 1,3-diarylidene thiourea (DAT) was examined as a new corrosion inhibitor for iron in 1 M hydrochloric acid solution.

Nonlinear electrochemical phenomenon, a potential perturbation signal by one or more sine waves will be generated current responses at more frequencies than the frequencies of the applied signal[126]. Current responses can then be measured, for example, at zero, harmonic, and intermodulation frequencies. This simple principle offers various possibilities for corrosion rate measurements, like the intermodulation or electrochemical frequency modulation (EFM) technique in which the potential perturbation

Introduction

signal consists of two sine waves of different frequencies. With this novel EFM technique, the corrosion rate can be determined from the corrosion system responses at the intermodulation frequencies. With the EFM technique a corrosion rate can be obtained instantaneously, without prior knowledge of the so-called Tafel parameters. The EFM approach requires only a small polarizing signal, and measurements can be completed in a short period. A special advantage of the EFM technique is its capability of inherent data validation control using “causality factors” (parameters introduced for the first time in this paper). It is shown that the EFM technique can be used successfully for corrosion rate measurements under various corrosion conditions, such as mild steel in an acidic environment with and without inhibitors and mild steel in a neutral environment.

The electrochemical behavior of Cu, Cu–37Zn and Zn in benzotriazole (BTA) containing chloride solutions was studied and compared using potentiodynamic, cyclic voltammetry and electrochemical impedance spectroscopy [127]. The presence of BTA in the chloride-containing solutions gave rise to higher breakdown potentials, significantly higher polarization resistances and inhibited the formation of CuCl_2 and zinc-containing corrosion products. These effects were observed for pure Cu, Cu–Zn and to a somewhat lesser extent pure Zn. The electrochemical impedance data were consistent with the formation of a polymeric BTA-containing layer for all three systems.

The electrochemical behavior of zinc in strong alkaline solutions containing 8.5 M of potassium hydroxide (KOH) and polymeric organic inhibitors was evaluated [128]. The concentrations of the organic inhibitors studies were in the range of 400–4000 ppm and included polyethylene glycol (PEG), with a molecular weight of 600, and polyoxyethylene alkyl

phosphate ester acid form (GAFAC RA 600). The electrochemical studies included anodic, cathodic, and linear polarization along with potentiostatic studies. It was found that the inhibition properties of PEG, in the strong alkaline solution, are by far much more efficient than the inhibition capability of GAFAC RA 600. Surface analysis obtained with the use of high resolution scanning electron microscopy (HRSEM) revealed different morphology characteristic developed at the zinc surface in the presence of the two inhibitors. A methodology employing electrochemical tests is proposed to quickly and conveniently evaluate inhibitors for Zn in alkaline media.

An examination of quantum chemical and corrosion inhibition studies were carried out to be investigated [129]. Whether any clear links exist between the results of quantum chemical calculations and the experimental efficiencies of urea (U), thiourea (TU), acetamide (A), thioacetamide (TA), semicarbazide(SC), thiosemicarbazide(TSC), methoxybenzaldehydethiosemicarbazone(MBTSC), 2-acetylpyridine-(4phenyl)thiosemicarbazone (2AP4PTSC) 2-acetylpyridine-(4-methyl)thiosemicarbazone (2AP4MTSC), benzointhiosemicarbazone (BZOTSC) and benzilthiosemicarbazone (BZITSC) being corrosion inhibitors. The quantum chemical calculations had been performed by using DFT, abolition molecular orbital and semi-empirical methods for some amides and thiosemicarbozone derivatives being corrosion inhibitors. The highest occupied molecular orbital energy (E_{HOMO}), lowest unoccupied molecular orbital energy (E_{LUMO}), the energy gap between E_{HOMO} and E_{LUMO} ($\Delta E = E_{\text{HOMO}} - E_{\text{LUMO}}$), dipole moments (μ), charges on the C, O, N and S atoms, the total energies of the molecules and the polarizabilities $\langle \alpha \rangle$, the coefficients of the development of the MO over the atomic orbital (AO) corresponding to the bond between atoms which a new bond is established had been

calculated. Results of quantum chemical calculations and experimental efficiencies of inhibitors were subjected to correlation analysis.

Electrochemical frequency modulation (EFM) technique, the non-linear behavior of a corroding system was measured. This non-linear behavior is likely to be different for a system undergoing uniform or pitting corrosion [130]. The implementation of the EFM technique to detect pitting corrosion has been investigated by observing the fluctuations in the so-called causality factors. These causality factors, resulting from an EFM test and in the ideal case having values of 2 and 3, respectively, are normally used for quality and data validation purposes. While investigating pitting corrosion, they showed different behavior leading to the CPT (critical pitting temperature) detection.

Inhibition of the corrosion of zinc in 0.01 to 0.04 M H_2SO_4 by erythromycin was studied using weight loss and hydrogen evolution methods [131]. The obtained results indicated that erythromycin is a good adsorption inhibitor for the corrosion of zinc in H_2SO_4 solutions. The inhibition efficiency of erythromycin increased with increasing concentration but decreased with the increase of temperature. Thermodynamic and adsorption studies reveal that the adsorption of erythromycin on zinc surface is exothermic, spontaneous and is characterized with increasing degree of orderliness. The adsorption characteristics of the inhibitor are best described by the Langmuir adsorption model. From the variation of inhibition efficiency with temperature and the calculated values of the activation and free energies (which are within the limits expected for physical adsorption).

The corrosion behavior for zinc in ($\text{HNO}_3 + \text{H}_2\text{SO}_4$) binary acid mixture containing ethanol amines was studied [132] . Corrosion rate increased with concentration of acid and temperature. At constant acid concentration, the inhibition efficiency of ethanol amines increased with the inhibitor concentration. Value of G_a increased and inhibition decreased with the increase of temperature. The mode of inhibition action appears to be chemisorption.